

NASA/TP—1998–208475



Electrodynamic Tether Propulsion and Power Generation at Jupiter

D.L. Gallagher and L. Johnson

Marshall Space Flight Center, Marshall Space Flight Center, Alabama

J. Moore

SRS Technologies, Huntsville, Alabama

F. Bagenal

University of Colorado, Boulder, Colorado

National Aeronautics and
Space Administration

Marshall Space Flight Center

June 1998

Available from:

NASA Center for AeroSpace Information
800 Elkridge Landing Road
Linthicum Heights, MD 21090-2934
(301) 621-0390

National Technical Information Service
5285 Port Royal Road
Springfield, VA 22161
(703) 487-4650

TABLE OF CONTENTS

1.	INTRODUCTION	1
2.	BACKGROUND	2
3.	TETHER PHYSICS AT JUPITER	3
4.	TETHER PROPULSION AND POWER MODEL	11
5.	JOVIAN CAPTURE ANALYSIS	12
6.	JOVIAN ELECTRODYNAMIC TETHER POWER GENERATION AND MANEUVERING CAPABILITY	16
7.	MISSION-SPECIFIC ISSUES	19
	7.1 Gravity Gradient Forces	19
	7.2 Micrometeoroid Threat	20
8.	SUMMARY	21
9.	RECOMMENDATIONS	23
	REFERENCES	24

LIST OF FIGURES

1.	Total electron density with constant density contours at 10, 100, 500, 1,000, 3,000, and 6,000 cm^{-3}	4
2.	Spacecraft speed relative to the Jovian magnetic field	5
3.	Induced EMF in a 10-km tether at Jupiter	6
4.	Tether current contours for 0.1, 0.5, 1, 5, 10, and 20 A	7
5.	Force experienced by the tether	9
6.	Total power developed in the tether	10
7.	Orbit footprint for Jovian orbit capture with 11.009-km bare-wire tether	13
8.	Tether propulsive force magnitude during capture maneuver	13
9.	Tether current and voltage during capture maneuver	14
10.	Orbit circularization using capture tether	15
11.	Power generation capability for 5-day elliptic orbit	16
12.	Effect of tether power generation forces on polar orbit	17
13.	Tether orbital maneuvering capability for changing apojove	18
14.	Tether orbital maneuvering capability for plane change	18
15.	A rotating spacecraft and tether system could be used to maintain tether tension	19
16.	The probability of survival for a single strand tether in near-Jovian space	20
17.	Artist's concept of an electrodynamic tether-augmented spacecraft at Jupiter	21

TECHNICAL PUBLICATION

ELECTRODYNAMIC TETHER PROPULSION AND POWER GENERATION AT JUPITER

1. INTRODUCTION

This report discusses the results of a study performed to evaluate the feasibility and merits of using an electrodynamic tether (EDT) for propulsion and power generation for a spacecraft in the Jovian system. The environment of the Jovian system has properties which are particularly favorable for utilization of an EDT. Specifically, the planet has a strong magnetic field and the mass of the planet dictates high orbital velocities which, when combined with the planet's rapid rotation rate, can produce very large relative velocities between the magnetic field and the spacecraft. In a circular orbit close to the planet, tether propulsive forces are found to be as high as 50 N and power levels as high as 1 MW.

Models were developed to simulate tether propulsion and power generation performance in the Jovian planetary environment. The simulation code was used to evaluate the use of an EDT for Jovian orbit insertion, orbital maneuvering once established in Jovian orbit, and spacecraft power generation. No attempt is made to optimize a tether design for a specific mission. Instead, the model was exercised in several generic scenarios intended to demonstrate the potential of an EDT for future engineering studies and mission planning. For all cases, the tether is assumed to be uninsulated and to have a 1-mm diameter. The length is specified as an input to the simulation and it is assumed that the tether is deployed radially.

2. BACKGROUND

In recent years, tethers have come to offer significant opportunities in many low-Earth orbit applications. Conducting and nonconducting tethers are being considered for electrical power and propulsion systems.¹ Conducting tethers or EDT's derive their properties as a result of the current flowing through a moving wire in a magnetic field and in the presence of a plasma or conducting medium. Tethers may be useful in any planetary system where there exists a magnetic field and a plasma through which current closure can occur.

But why Jupiter? The first inducement is the large Jovian magnetic field, much larger than that at the Earth. The real motivation, however, is the need for alternative power generation and propulsion techniques for future missions to Jupiter. Due to low solar luminosity, radioactive thermoelectric generators (RTG's) have been used for electrical power in all past deep space missions. The finite risk of releasing plutonium into the terrestrial environment may rule out RTG's on future missions. The possibility of using solar panels for electrical power generation has improved in recent years. Even with improvements in this technology, however, extended exposure to high levels of radiation in the Jovian system are expected to rapidly degrade the effectiveness of solar arrays. Extended operations in the Jovian system, or around any planet, also typically require use of an expendable propellant for orbital maneuvering. This may lead to high "wet" spacecraft mass at launch and/or limited lifetime on orbit. It is for these reasons, and because of the strong magnetic field and rapid planetary rotation, that electromagnetic tethers are being considered for use in the Jovian magnetosphere. Stion 3 reports the results of the assessment from a physics perspective. Stions 4-6 more specifically address the tether's use for spacecraft applications.

3. TETHER PHYSICS AT JUPITER

This section of the report discusses the initial results of analyzing the performance of an EDT in the Jovian planetary system. Tether modeling is based on results from the TSS-1R mission and the theories of Parker and Murphy² and Sanmartin.³ The computed tether performance represents maximum limiting current and resulting power estimates. The Jovian magnetic field model is obtained from Khurana,⁴ consisting of the Goddard Space Flight Center (GSFC) O₆ internal field model, and an Euler potential formulation for the external field. The plasma density model is a simplified version of that presented by Bagenal⁵ and consists of a spherically symmetric distribution, plus an Io torus. The results also depend on several assumptions. The electron temperature, which is used to estimate the thermal current to the tether is assumed to be 10 eV. Inside of 5 Jovian radii (R_J), the electron temperature is only a few electron volts and outside of this distance, it is 10–50 eV. This means the estimated current will be somewhat high inside this distance, and low outside this distance. Tether current varies with the square root of the thermal electron temperature, therefore, it is not tremendously sensitive to it. A tether length of 10 km has been assumed, along with a cylindrical tether of 1-mm diameter.

The analysis of EDT performance is accomplished in two coordinate systems. One is the System III (1965) coordinate system, which rotates with the Jovian magnetic field. Both the magnetic field and density models are defined in this coordinate system. The second is an inertial coordinate system, where the z axis is along the planetary spin axis. Due to the preliminary nature of this study, no effort has been made to orient the x axis of this inertial coordinate system toward the first point of Aries or any other inertial reference point. All results are shown graphically in the x-z plane of this work's inertial coordinate system. Each of the displays extend ±8 R_J along the x and z axes and show constant level contours of various quantities.

Figure 1 shows total electron density with constant density contours at 10, 100, 500, 1,000, 3,000, and 6,000 cm⁻³. It is made up of three components: inside the Io torus, the Io torus, and outside the torus. Inside and outside the torus, the density falls off exponentially. Inside the torus, the density is derived from linear interpolations of a measured radial profile. The torus falls off exponentially away from the magnetic equator.

Induced tether current will depend upon the speed with which the tether moves through the Jovian magnetic field. That speed will depend on spacecraft motion around the planet, \vec{v}_{sc} , and planetary rotation, \vec{v}_j . For the purpose of initially exploring tether behavior, the spacecraft motion is assumed to result from a circular orbit at each radial distance and latitude where the calculations are made:

$$\vec{v}_{sc} = \left(\frac{GM_J}{r} \right)^{\frac{1}{2}} \left(-\sin(\theta)\hat{\theta} + \cos(\theta)\hat{\phi} \right) , \quad (1)$$

where θ is the latitude and ϕ is the longitude. This velocity is added to the velocity of a stationary location relative to planetary rotation, given by

$$\vec{v}_j = -1.7585 \cdot 10^{-4} \cdot r \cos(\theta) \hat{\phi} . \quad (2)$$

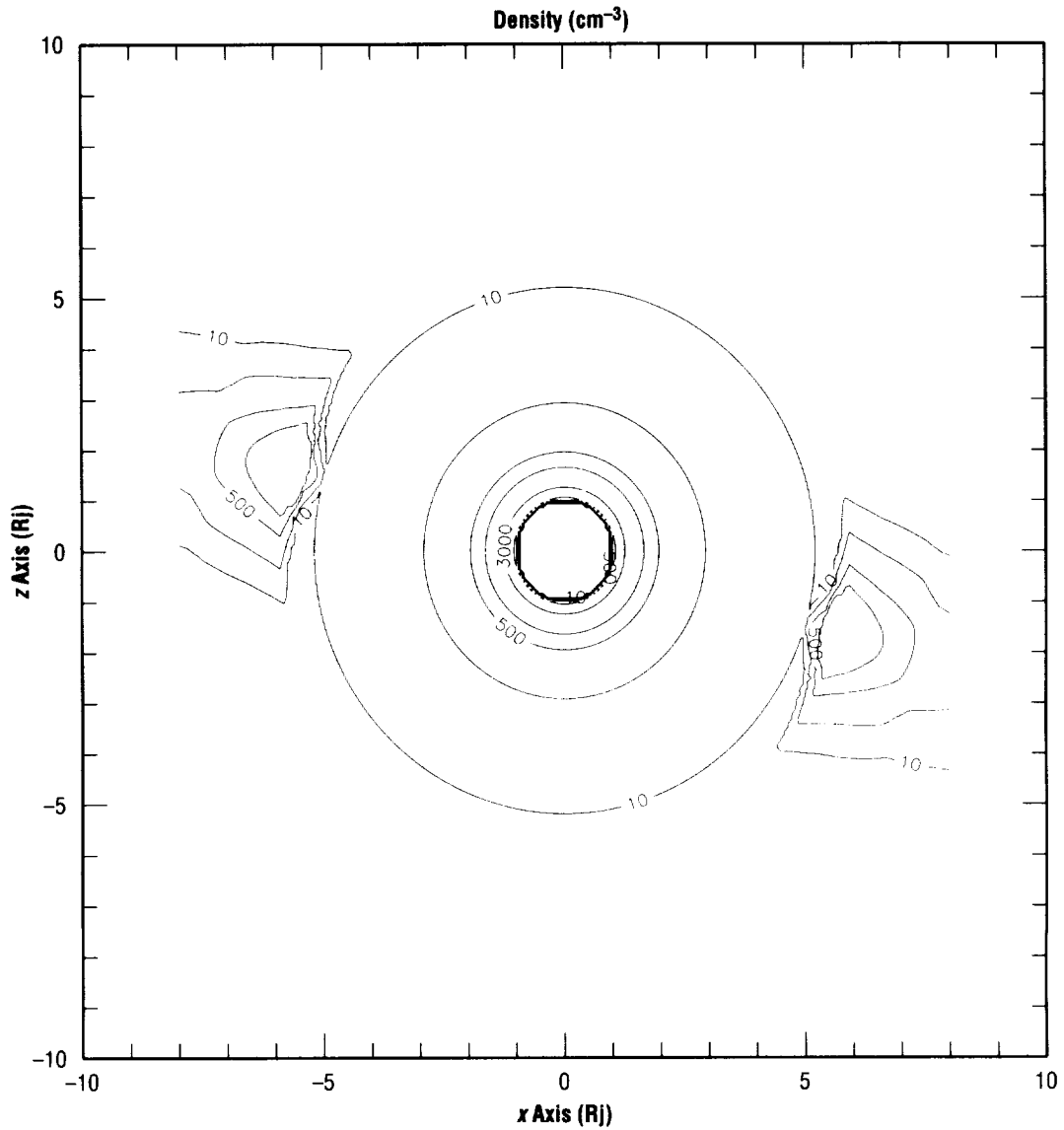


Figure 1. Total electron density with constant density contours at 10, 100, 500, 1,000, 3,000, and 6,000 cm^{-3} .

Jupiter is assumed to rotate with a period of 9 hr 55 min 29.70333 s. The resulting speed of the spacecraft relative to the planetary magnetic field, \vec{v}_{rel} , which is the sum of spacecraft speed and planetary rotation, is plotted in figure 2. Constant velocity contours are shown for 1, 2, 4, 6, 8, 10, 20, and 40 km/s

$$\vec{v}_{rel} = \vec{v}_{sc} + \vec{v}_j . \quad (3)$$

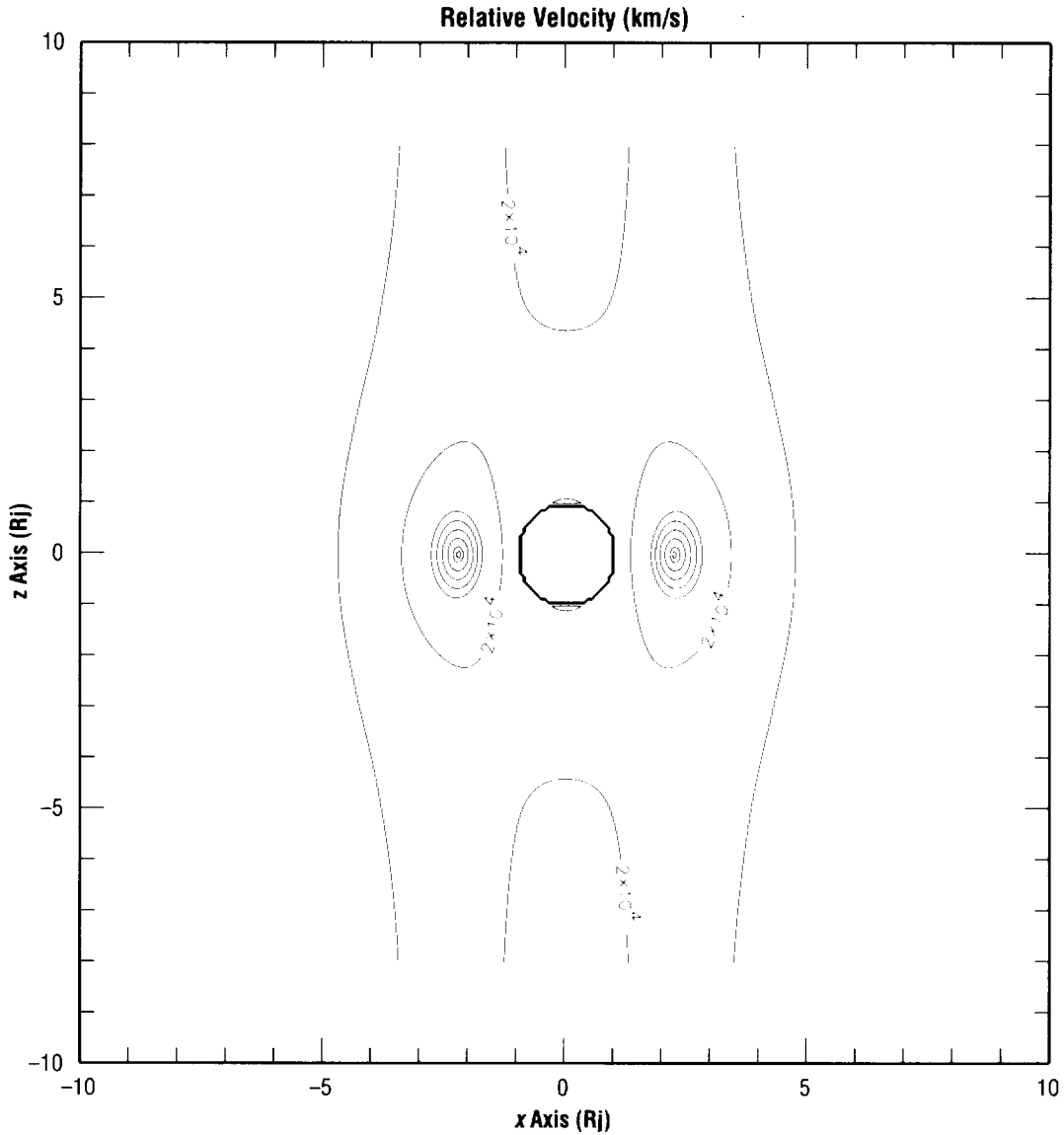


Figure 2. Spacecraft speed relative to the Jovian magnetic field.

You can see that for most locations, the planetary rotation dominates the plotted speed, i.e., it increases with increasing distance. Close to the planet, the orbital spacecraft speed begins to dominate over the planetary rotation. At 90 degrees, the planetary motion is not a factor, leaving only the orbital motion to contribute to induced electromagnetic force (EMF) in the tether.

Figure 3 shows induced EMF in the 10-km tether. Contours are shown for -50, -10, -1, -0.1, 0.1, 1, and 10 kV values. Induced voltage depends upon the tether length, \vec{l} , the velocity relative to the magnetic field, \vec{v}_{rel} , and the vector magnetic field, \vec{B}

$$V = \vec{l} \cdot \vec{v}_{rel} \times \vec{B} . \quad (4)$$

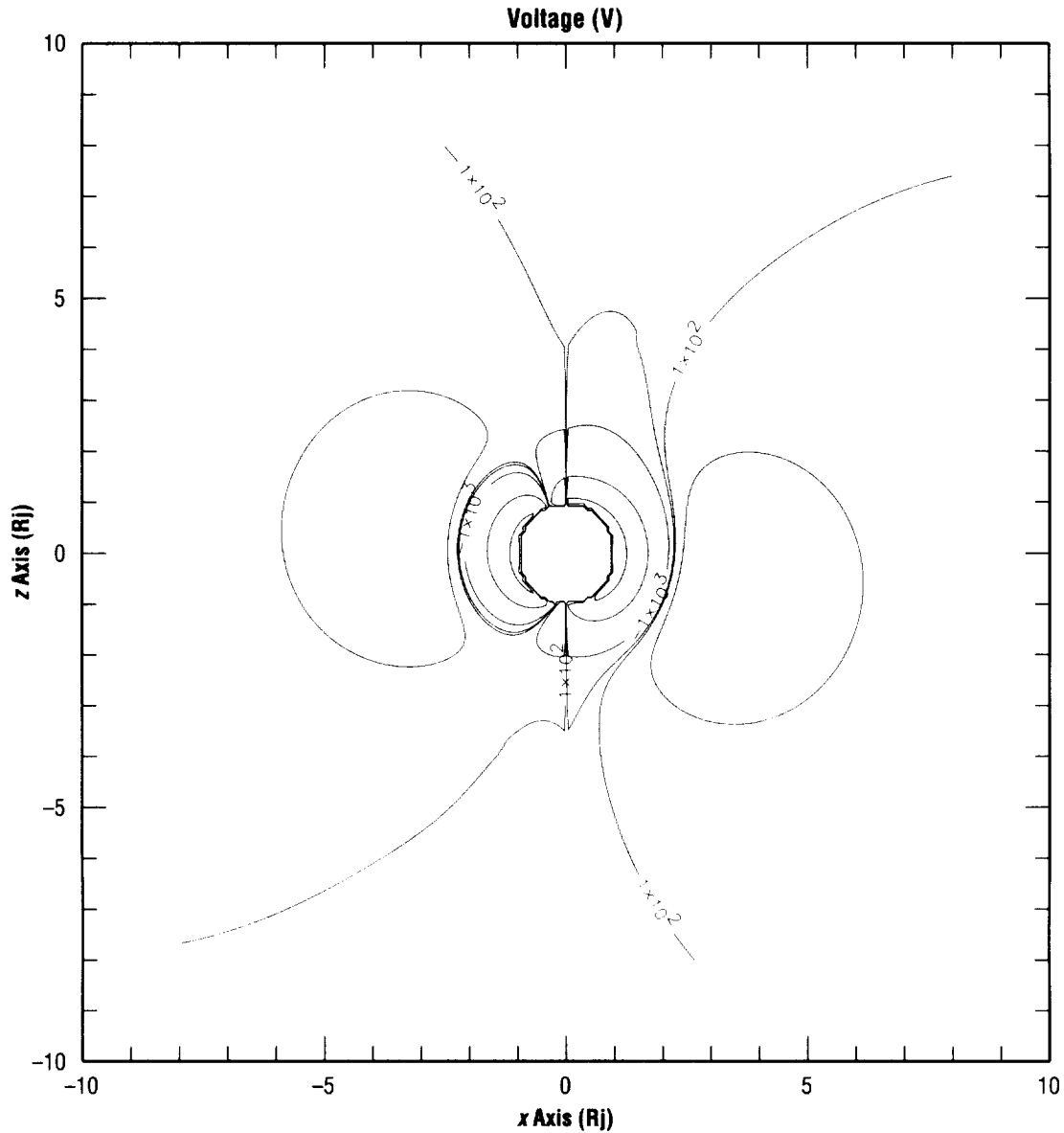


Figure 3. Induced EMF in a 10-km tether at Jupiter.

Tether current is plotted in figure 4. Here, contours are shown for 0.1, 0.5, 1, 5, 10, and 20 A. Based on Parker and Murphy,² current into a conductor in a magnetic field is equal to the thermal current, I_0 , times a factor. The factor is a function of induced voltage, V ; the area of the conducting surface, a , and the magnetic field strength, B . The thermal current is a function of the cross-sectional area of the conducting surface and the component of the thermal current density along the magnetic field. Thermal current density, j_0 , is a function of the density, n_e , the mean thermal electron velocity, v_{Te} , and the charge of an electron, e ,

$$j_0 = \frac{en_e v_{Te}}{4} . \quad (5)$$

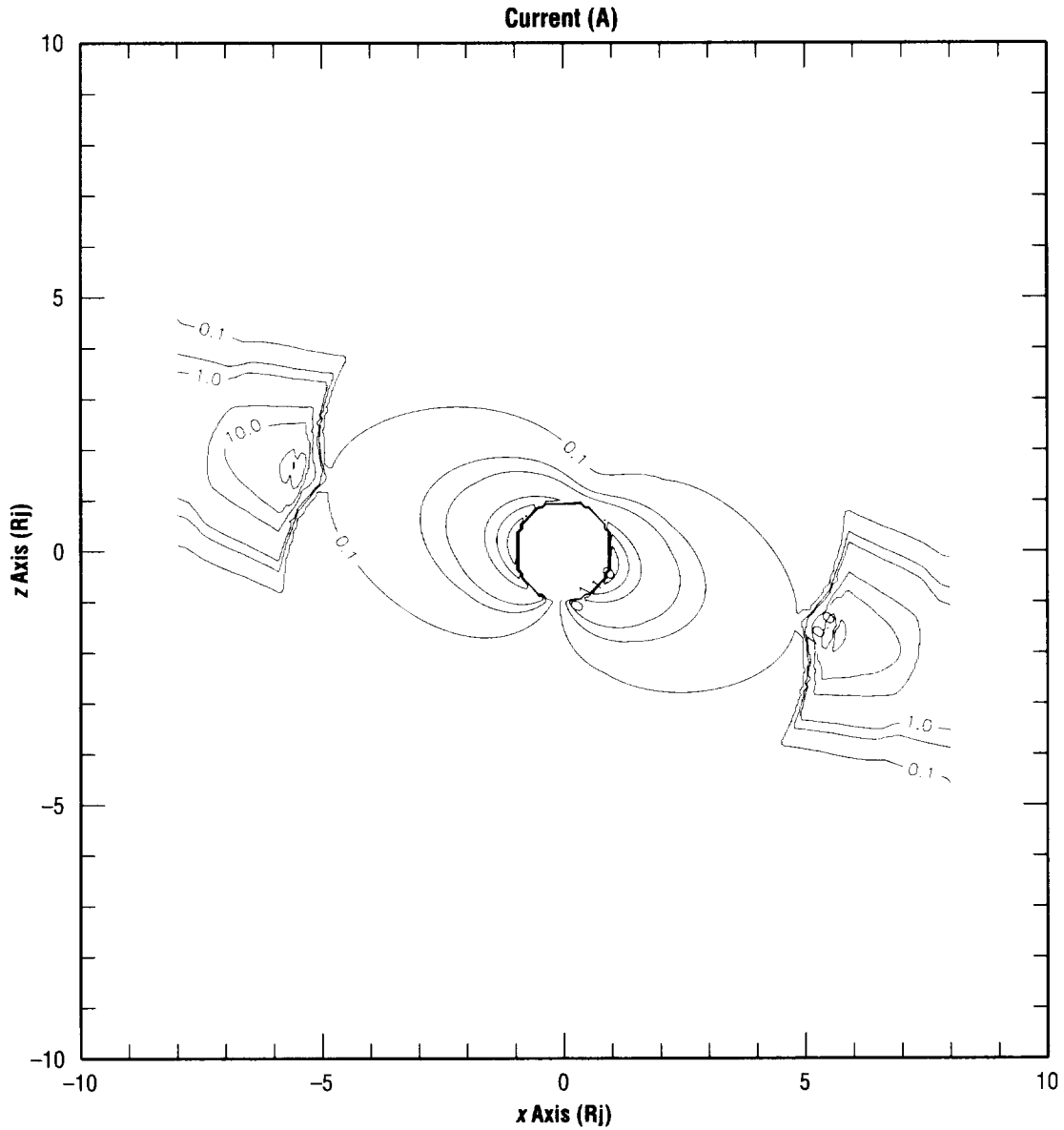


Figure 4. Tether current contours for 0.1, 0.5, 1, 5, 10, and 20 A.

The component of the current density along the magnetic field is obtained by taking one-fourth of the total thermal current density. The area of the conducting surface is taken to be the area of the tether projected onto a plane transverse to the magnetic field

$$a = d \cdot l \cdot \sin(\alpha) \quad , \quad (6)$$

where d is the diameter of the tether (0.001 m), l is the tether length (10^4 m), and α is the angle between the radial tether and the vector magnetic field. This angle is obtained from

$$\alpha = \cos^{-1}\left(\frac{B_r}{B}\right) \quad , \quad (7)$$

where B_r is the radial component of the Jovian magnetic field. The thermal current is multiplied by a factor of 2 to take into account the collection of current from both the parallel and antiparallel directions along the magnetic field

$$I_o = 2 \cdot a \cdot j_o \quad . \quad (8)$$

Finally, the current is multiplied by factors of 2.5 and 30. The limiting current into a tether was found to be a factor of 2–3 times greater than Parker and Murphy² in the TSS and TSS–1R missions, which is the source of the first factor. The sond factor results from the analysis of bare tether performance, which is thought to enhance the current collection by a factor of at least 30 over the spherical end-collector used in the TSS and TSS–1R missions⁶

$$I = 75I_o \left(1 + \left[4.56 \times 10^{-3} \frac{V(\text{volts})}{a^2(\text{meters}^4) B^2(\text{gauss}^2)} \right]^{\frac{1}{2}} \right) \quad . \quad (9)$$

The force, \vec{F} , a current-carrying tether would experience is shown in figure 5, with contours at 0.01, 0.05, 0.1, 0.5, 1, 5, 10, 25, and 50 N. The force is obtained from the tether length, l ; current, \vec{I} ; and the magnetic field, \vec{B} ,

$$\vec{F} = l\vec{I} \times \vec{B} \quad . \quad (10)$$

Figure 6 shows the power developed in a current-carrying tether. Contours are drawn for even decades from 1 W to 10 MW. Power is simply obtained from the product of the induced EMF and the current

$$P = V \cdot I \quad . \quad (11)$$

The orbital distance of Europa puts it beyond the distance treated in this report; however, it is clear that tether performance will be limited at that distance unless plasma density is enhanced locally by the presence of a Europa atmosphere.⁷

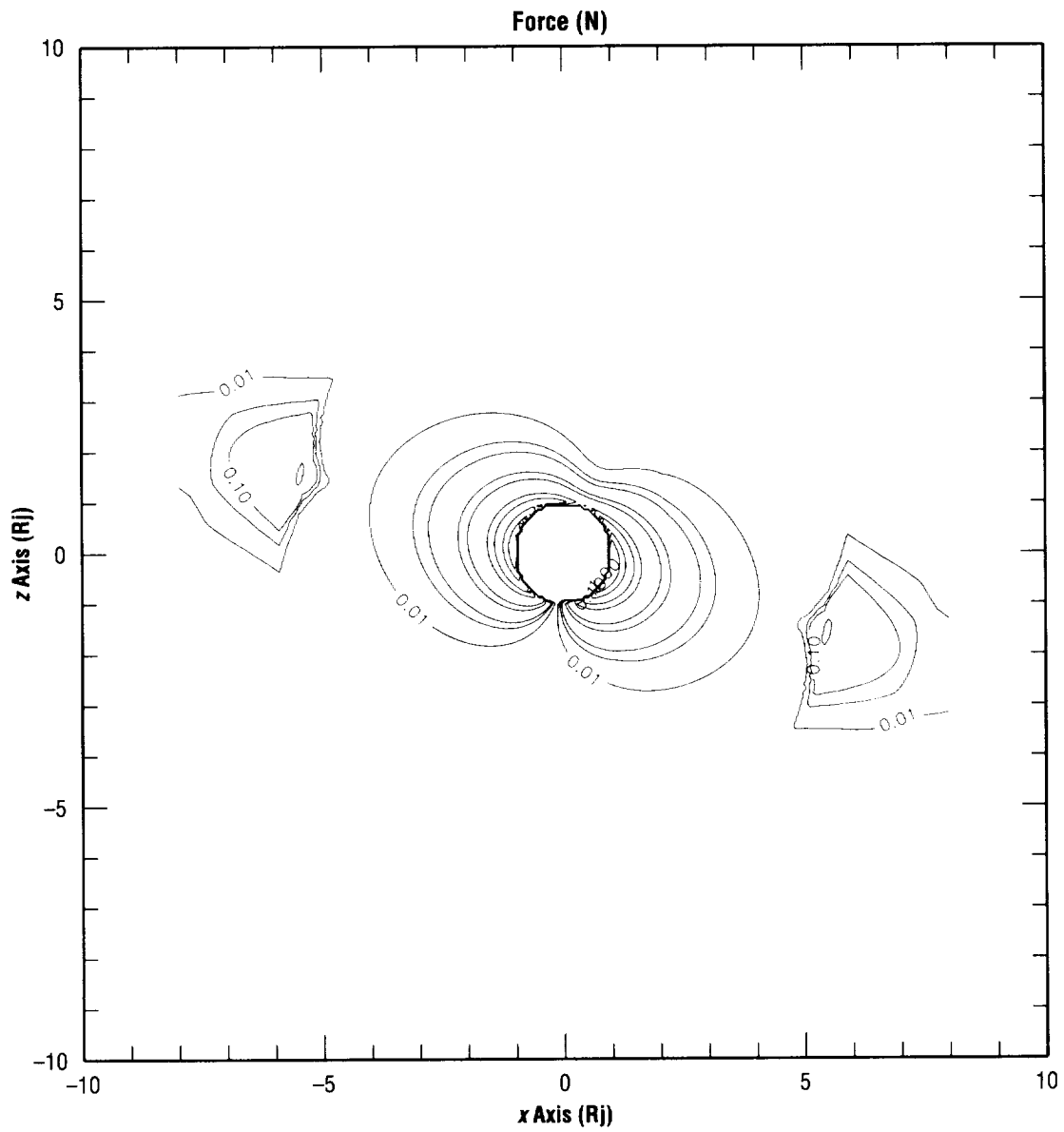


Figure 5. Force experienced by the tether.

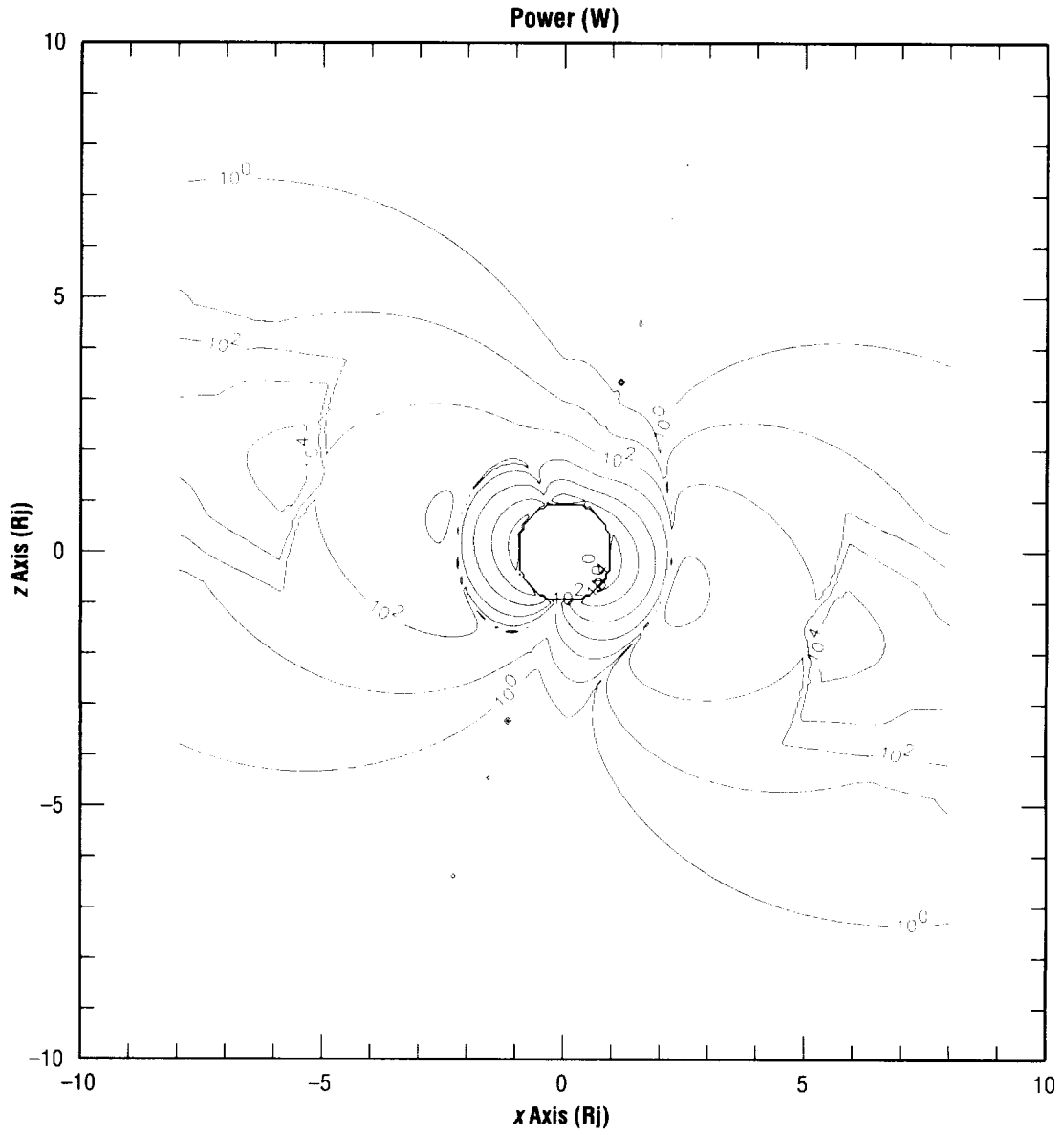


Figure 6. Total power developed in the tether.

4. TETHER PROPULSION AND POWER MODEL

The simulation developed for this study consists of a fifth-order, 3 degrees of freedom spacecraft trajectory model coupled with an EDT model. The trajectory model propagates the spacecraft's state, from user-specified initial conditions, by solving the two-body equations of motion in the following form:

$$d^2\mathbf{r} / dt^2 = -m\mathbf{r} / r^3 + \mathbf{a}_t \quad , \quad (12)$$

where

\mathbf{r} = spacecraft position vector

m = gravitational constant

t = time

\mathbf{a}_t = acceleration caused by tether forces.

The position and acceleration vectors are specified in a Cartesian inertial coordinate system. The model uses a fifth-order Runge-Kutta algorithm with automatic stepsize control to integrate the equations of motion. At each time step, the trajectory code passes the current state vector ($x, y, z, V_x, V_y, V_z, t$) to the tether model. The tether model then calculates the electrodynamic voltage, current, and force vector resulting from the motion of the conducting tether relative to the Jovian magnetosphere. The force vector is passed back to the trajectory model and used to calculate \mathbf{a}_t in equation (1) by dividing by the mass of the spacecraft. The simulation continues over the user-specified time period. Spacecraft position and velocity are output at user-specified time increments as are tether performance parameters including tether propulsive forces, current, and voltage.

5. JOVIAN CAPTURE ANALYSIS

The tether simulation was initially used to evaluate the feasibility of using an EDT as an alternative to chemical propulsion or aerobraking for initial Jovian orbit insertion (JOI) of an interplanetary spacecraft. The use of a tether for this function is particularly appealing because of the large percentage of spacecraft mass required to perform this maneuver when using conventional propulsion systems. Additionally, the tether has the potential to be used for on-orbit maneuvering and/or power generation once the capture maneuver is completed. Thus, the weight of the tether can be traded against multiple systems of the spacecraft.

For the purpose of this study, it was necessary to make some assumptions regarding the spacecraft and mission. Typical spacecraft size and orbital requirements were evaluated by reviewing the requirements outlined in the "Jupiter Close Polar Orbiters: Preliminary Mission Studies"⁸ report. This report provides preliminary mission planning for two missions involving spacecraft in polar orbits around Jupiter. The proposed missions are the Radio Science Observer and the Auroral Observer. The first mission utilizes an orbit with perijove of 1.01 R_J and a period of 100 days. The sond mission utilizes an orbit with perijove of 1.05 R_J and a period of 5 days. The spacecraft mass was assumed to be 340 kg, which is consistent with the proposed polar orbiter spacecraft. It was assumed that the spacecraft would be launched in the low energy launch opportunity occurring in 2006. On arrival at Jupiter, the spacecraft has a predicted hyperbolic excess velocity of 6.854 km/s.

For the capture analysis, the simulation code was used to evaluate the feasibility of capturing a spacecraft from an Earth-Jupiter transfer orbit directly into a 1.05 R_J perijove by a 100-day orbit. The constraint for a polar orbit was not enforced in order to allow the spacecraft to utilize the maximum benefit from the rotation of the planet's magnetosphere. The arrival trajectory was targeted to enter a retrograde equatorial orbit. The simulation was initialized by specifying the initial conditions of the spacecraft on a point along the hyperbolic approach trajectory inbound toward the planet. Tether length was varied parametrically and the resulting orbits were evaluated. It was found that the desired orbit could be established using a tether length of 11.009 km (subject to the previously stated assumptions; bare wire tether, radially deployed, 1-mm diameter). Figure 7 shows the footprint of the spacecraft's trajectory. The simulation begins with the spacecraft at a distance of 6 R_J from the planet's center on the hyperbolic approach trajectory. As the spacecraft approaches, the planet tether forces increase, decelerating it. The simulation is continued for 8.64×10^6 s (100 days). Figure 7 shows that the spacecraft is captured into the desired elliptic orbit. The propulsive force generated by the tether during the capture maneuver is illustrated in figure 8. The figure shows that the tether force is applied over a short period of time during the initial flyby. The tether force drops off rapidly once the spacecraft is more than approximately 2.5 R_J from the planet's center. Once the tether approaches the planet, the tether force builds rapidly to a peak of 107 N and then drops rapidly as the spacecraft moves away from the planet.

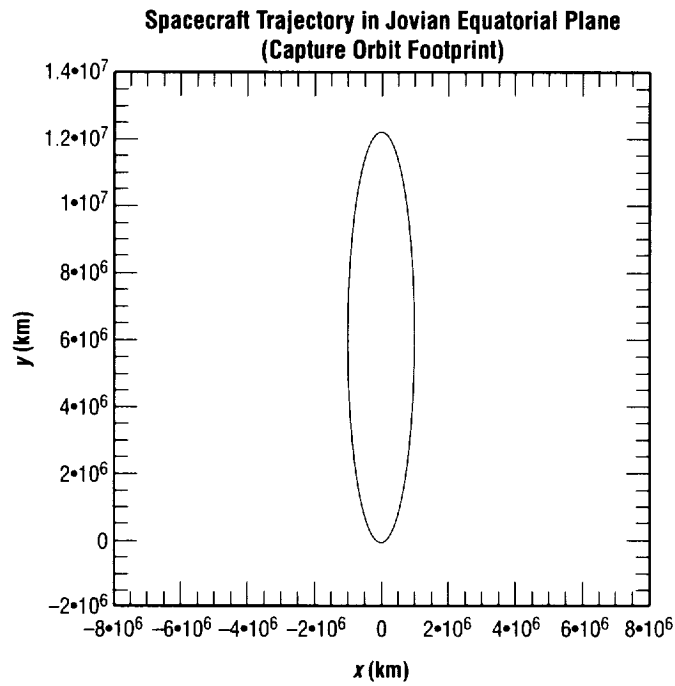


Figure 7. Orbit footprint for Jovian orbit capture with 11.009-km bare-wire tether.

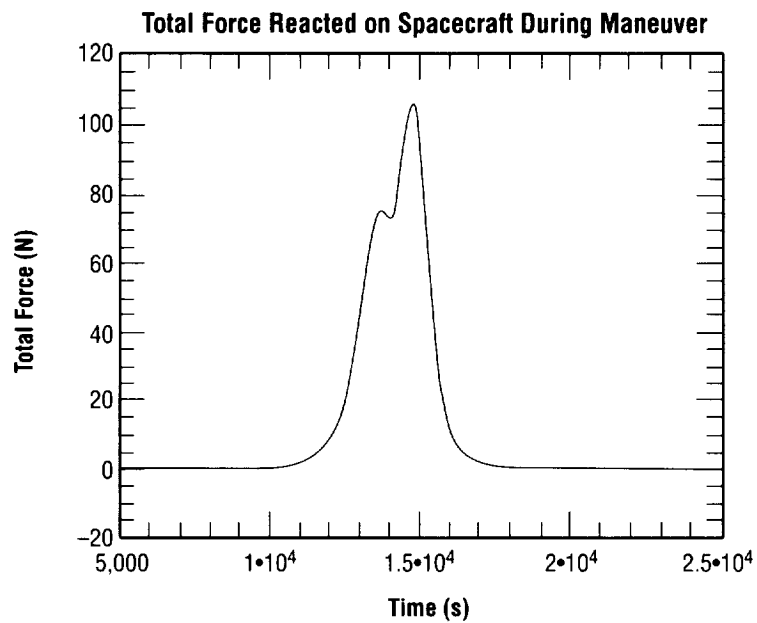


Figure 8. Tether propulsive force magnitude during capture maneuver.

Tether voltage and current during the encounter are shown in figure 9. The voltage peaks at approximately 290,000 V and the current peaks at 26.5 A. The peak power generation during the encounter is approximately 6.6 MW. These current and power levels exceed the power-carrying capabilities of reasonably sized (diameter) tethers constructed of conventional materials. Additionally, the large propulsive forces generated by the tether would preclude gravity-gradient stabilization of the tether, which is implied by the assumed radial orientation of the tether. A first-order estimate of tether tension required for stability in this fly-by encounter is 130 N. These results indicate that based on the physics-orbit capture, using a tether is possible; however, it seems that engineering problems would probably preclude the use of a tether for orbit capture in most mission scenarios. It may be possible to reduce the peak forces and power somewhat by targeting for a higher perijove radius which would increase the fly-by time and reduce the peak electron density during the encounter. Additional analysis is required to fully investigate this possibility. The tether stability problem could probably be addressed by designing the spacecraft for spin stabilization by splitting the spacecraft mass into two endmasses and spinning the system to produce tension. Practical solutions to the high power levels have not been readily identified. However, it should be noted that it might be possible to justify the weight of a tether system engineered for these power levels if the spacecraft had a requirement for a very large power supply.

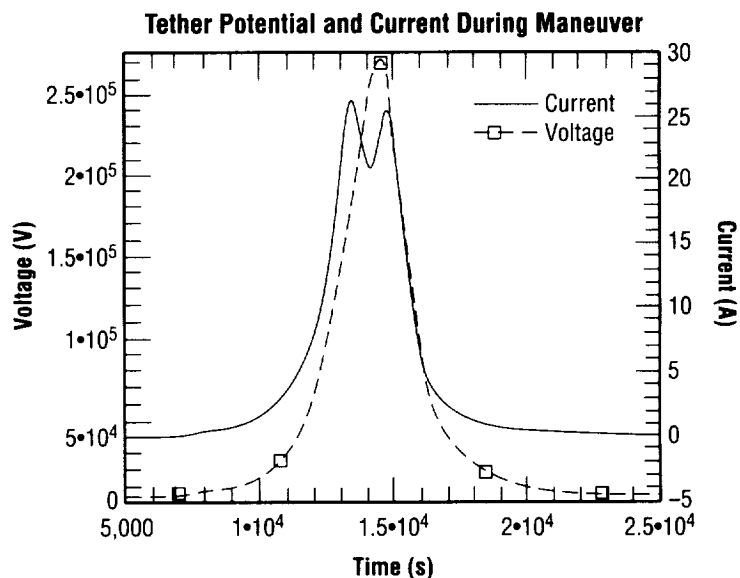


Figure 9. Tether current and voltage during capture maneuver.

Some additional interesting observations resulted from the capture analysis. It was noted that, if the power produced during the fly-by could be captured with some form of rapid charge rate device and then utilized at a lower discharge rate, an average power of 1,731 W could be supplied to the spacecraft during the 100-day initial orbit period. It was also noted that a tether sized for orbit capture would have significant orbital maneuvering and power generation capabilities for use in subsequent orbits. Figure 10 shows the capability of the capture tether (11.009 km) to circularize the spacecraft (340 kg) orbit after the initial fly-by. The orbit can be circularized to a radius of 1.05 R_J approximately 120 days after the initial fly-by with no propellant required for circularizing.

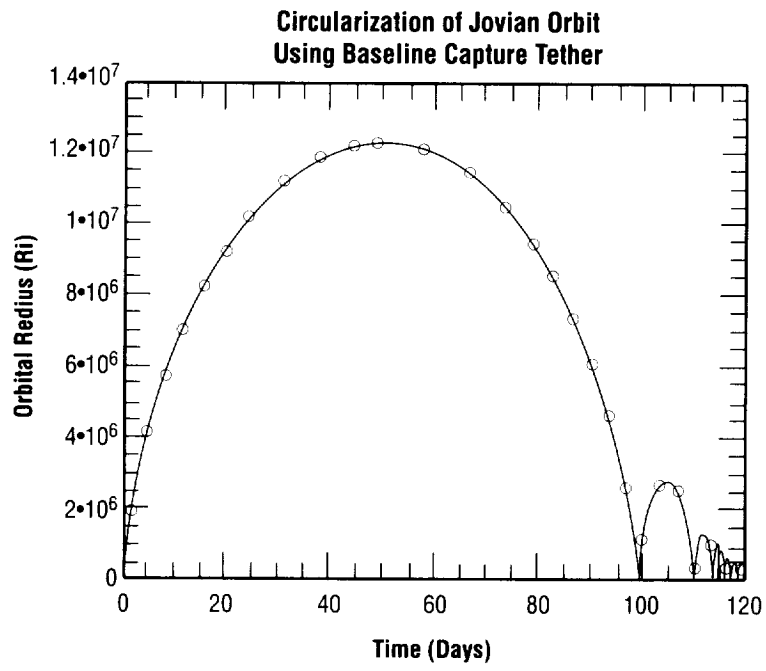


Figure 10. Orbit circularization using capture tether.

6. JOVIAN ELECTRODYNAMIC TETHER POWER GENERATION AND MANEUVERING CAPABILITY

The Jovian tether model was also used to investigate the use of EDT's for power generation and orbital maneuvering once established in a specified Jovian orbit. A tether was sized to address the power requirements of a mission similar to the Radio Science Observer. The spacecraft was modeled in a polar orbit with a $1.01 R_j$ perijove and 5-day period. A tether was sized to provide a time-averaged power supply of 180 W over the 5-day orbit (21,600 Whr/orbit). It was determined that a $4.75\text{-km} \times 1\text{-mm}$ tether could meet this requirement. The elliptic orbit and low perijove radius of this orbit result in an impulsive power generation profile with a high rate and short period similar to the profiles shown for the capture maneuver. However, the shorter tether length required for this application results in much more manageable peak power levels. The peak power generation rate for the tether described above is 140 kW. Storage of the power for use over the entire orbit would require a high charge rate storage device. Figure 11 shows the time-averaged power generation capability of the tether described above for various different orbit inclinations. The power generation capability of the tether increases significantly as the orbit inclination is varied from polar to retrograde equatorial. The figure demonstrates that a much shorter ($<4.75\text{ km}$) tether could be used to meet the spacecraft power requirements for other orbital inclinations.

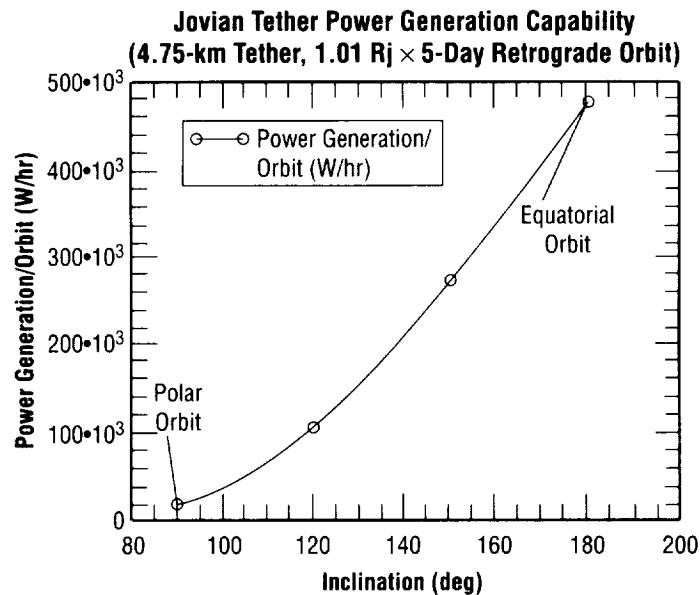


Figure 11. Power generation capability for 5-day elliptic orbit.

The sensitivity of power generation to orbit inclination is primarily a function of the orientation of the tether (radial) with respect to the planet's magnetic field. It was noted that if the tether was spin stabilized it would be possible to orient the tether in any inertial plane desired. In that case, it might be possible to meet the spacecraft power requirement with a tether much shorter than indicated by this analysis.

Typically, EDT power generation results in a propulsive drag force, which affects the motion of the spacecraft. The propulsive force can be desirable or undesirable depending on the specific mission objectives. Figure 12 shows the effect of tether power generation over time on the $1.01 R_j \times 5$ -day polar orbit used to size the power generation tether described above. The tether forces resulted in only a slight lowering of the apojove radius over the 100-day period simulated. It was also noted that the amount of apojove decay varied from orbit to orbit. This is possibly due to the inclination of the pole and the time phasing of different orbit passes with the rotation of the planet.

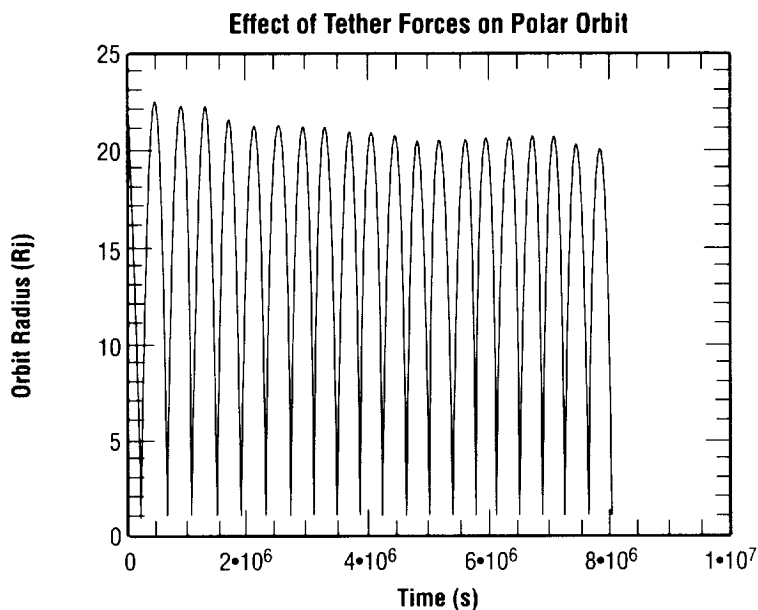


Figure 12. Effect of tether power generation forces on polar orbit.

The rapid rotation rate of Jupiter is one of the unique properties of the Jovian system that broadens the potential applications of EDT's for Jovian missions. For example, in a posigrade orbit the direction of the tether propulsive force can vary by as much as 180 degrees, depending on the altitude of the orbit. At high altitudes, the rotational velocity of the magnetic field dominates the relative velocity and, conversely, at low altitudes, the spacecraft velocity dominates the relative velocity.

The forces resulting from the EDT can be exploited for orbital maneuvering. The orbital maneuver capabilities of the 4.75-km tether are illustrated in figures 13 and 14. These figures were generated from the simulation results generated in the power generation study. Figure 13 shows the rate of apojove change predicted as a function of orbit inclination. A maximum rate of 1.15 R_j per orbit is predicted for the case of a retrograde equatorial orbit. The peak power generation rate corresponding to this maneuvering rate is 895 kW. Figure 14 shows the plane change rate generated by the 4.75-km tether on the 340-kg spacecraft. A maximum plane change rate of 0.041 degree per orbit is predicted. Thus, for the cases studied, it appears that the tether is much more effective in performing in-plane orbital maneuvers. This is probably due to the very high spacecraft velocities near perigee in the elliptic orbits studied. The tether would probably be more effective for plane changes in a low circular orbit.

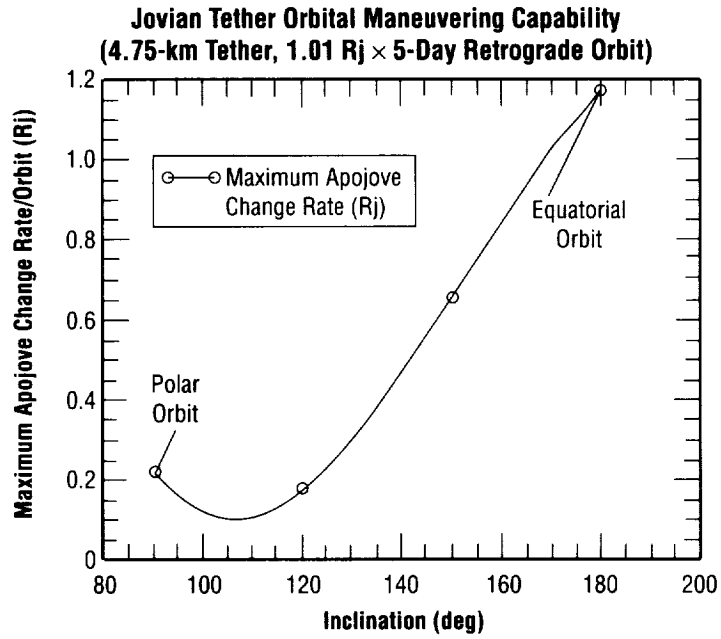


Figure 13. Tether orbital maneuvering capability for changing apojoive.

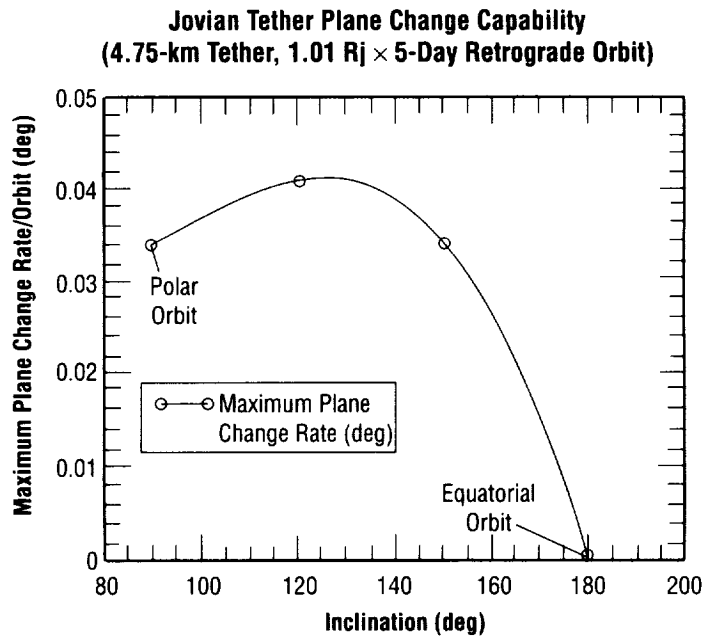


Figure 14. Tether orbital maneuvering capability for plane change.

7. MISSION-SPECIFIC ISSUES

7.1 Gravity Gradient Forces

In order to maintain tension in the tether sufficient to keep it vertical under the potentially tremendous forces experienced by operation near Jupiter, some mechanism other than gravity gradient stabilization must be used. In Earth-orbit gravity, gradient forces sufficient to keep the tether vertical and stable can be attained with relatively modest tether lengths and endmass weights. Due to the mass distribution of Jupiter, however, such forces are simply too weak.

One approach to keeping the tether vertical would be to include a stiffener to rigidize the tether after deployment. Another option would be to reevaluate the entire mission approach, making the tether an integral part of the design and potentially expanding the science scope of a mission to include multipoint science measurements using a rotating tether system and two small spacecraft. Such a system might look something like that illustrated in figure 15. The system's rotation keeps the tether from developing slack. This approach would also increase the potential science return because measurements could now be made in two places simultaneously, providing time-varying and spatially-varying time-coordinated observations.

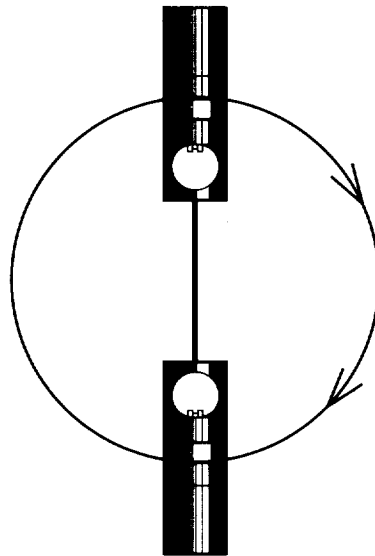


Figure 15. A rotating spacecraft and tether system could be used to maintain tether tension.

7.2 Micrometeoroid Threat

The threat of severing the tether by collision with a micrometeoroid is very real, as is the case with all tethers operating in Earth orbit. With an impactor of one-third the tether diameter assumed to cause a cut, the probability of survival for tethers of 1- and 10-mm diameter is shown in figure 16. Impactor diameters of one-third and one-fifth the tether diameter were assessed.

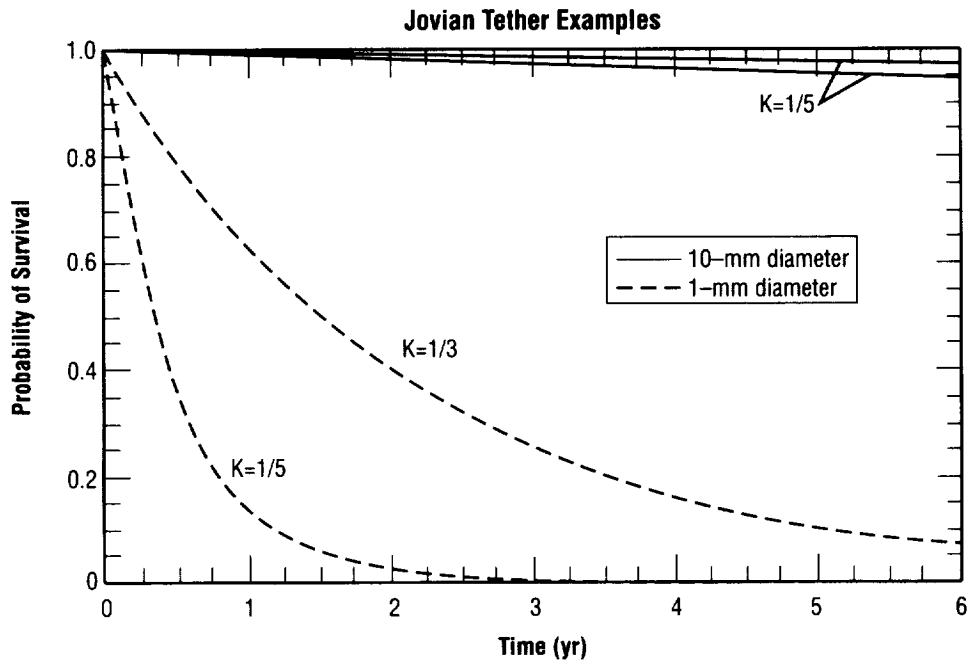


Figure 16. The probability of survival for a single strand tether in near-Jovian space.

8. SUMMARY

The use of EDT's in the Jovian system, as shown in the artist's concept (fig. 17), presents entirely new challenges and opportunities. In a circular orbit near the planet, it appears that induced tether voltages can reach as high as 50,000 V, currents can become greater than 20 A, power levels can reach over a million watts, and propulsive forces can reach higher than 50 N. Utilizing this tremendous power is clearly beyond current engineering capabilities.

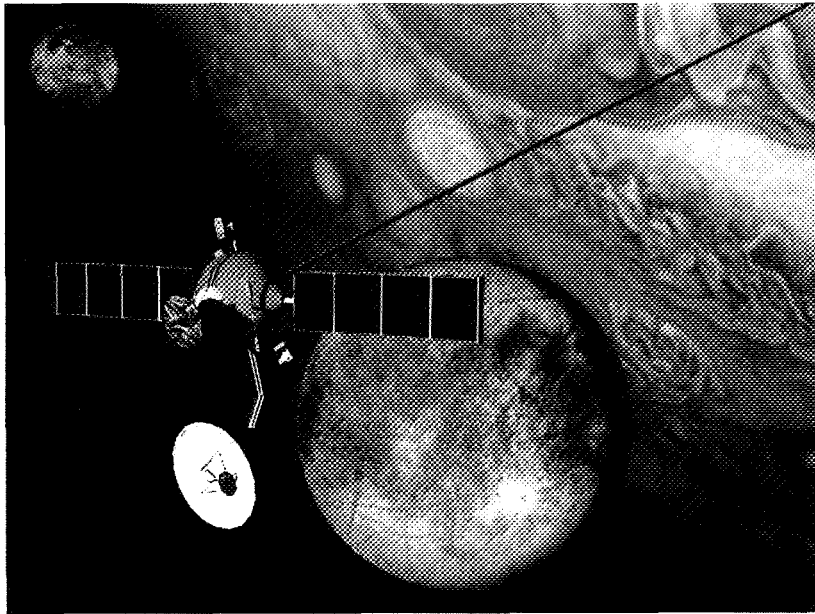


Figure 17. Artist's concept of an electrodynamic tether-augmented spacecraft at Jupiter.

EDT's appear, on the basis of plasma physics, to be feasible for use in the Jovian magnetosphere. They also appear to present significant engineering challenges including:

- High levels of tether current mean that managing a spacecraft system's thermal budget is not simple.
- The complex geometry of forces that a tether would experience around Jupiter means that sophisticated control of tether current will be required in order to achieve specific mission orbital characteristics.
- The capture analysis illustrates the potential for reasonably sized tethers to generate significant propulsive forces and tremendous, megawatt-level power generation.
- The huge power levels predicted for the capture maneuver would require a relatively heavy tether system to handle the load. However, the weight of such a system could be justified for missions with very large power requirements.

- It also appears feasible that very short tethers (~1 km) could be utilized for generating substantial power and orbital maneuvering capabilities. Power generation via tether may provide a realistic alternative to RTG's.
- The issue of tether stability remains open. Gravity gradient forces at Jupiter are insufficient to maintain tether orientation and tension under these propulsive loads. Alternative configurations, including a rotating system, should be considered.
- Additional analyses should be performed to evaluate the behavior of a tether system in lower altitude, more circular orbits. In these types of orbits it would be possible to provide continuous power and propulsive forces without the requirement to deal with the very large peak levels generated in highly elliptic orbits.

9. RECOMMENDATIONS

Based on the study performed to evaluate the feasibility and merits of using an EDT for propulsion and power generation for a spacecraft in the Jovian system, recommendations are as follows:

- A more specific and detailed characterization of EDT performance for propulsion and power generation should be performed using mission-specific requirements.
- A rotating system with two spacecraft connected by a small-to-modest length tether should be investigated. This should be closely coordinated with the science investigation team to optimize both the tether engineering and the enhanced science return.
- Power management options should be examined in more detail to determine the limits of both the tether and the power system.
- A detailed dynamic simulation should be developed to thoroughly understand the unique dynamic environment at Jupiter.
- Better physics models describing the plasma environment at Jupiter should be obtained and integrated into the simulations.

REFERENCES

1. Johnson, L., et al.: "Electrodynamic Tethers for Reboost of the International Space Station and Spacecraft Propulsion," AIAA-96-4250, 1996 AIAA Space Program and Technologies Conference, Huntsville, AL, September 24-26, 1996.
2. Parker, L.W.; and Murphy, B.L.: "Potential Buildup of an Electron-Emitting Ionospheric Satellite," *Journal of Geophysical Research*, Vol. 72, pp. 1631-1636, 1967.
3. Sanmartin, J.R.; Martinez-Sanchez, M.; and Ahedo, E.: "Bare Wire Anodes for Electrodynamic Tethers," *Journal of Propulsion and Power*, Vol. 9, pp. 353-360, 1993.
4. Khurana, K.K.: "Euler Potential Models of Jupiter's Magnetospheric Field," *Journal of Geophysical Research*, Vol. 102, pp. 11295-11306, 1997.
5. Bagenal, F.: "Empirical Model of the Io Plasma Torus: Voyager Measurements," *Journal of Geophysical Research*, Vol. 99, pp. 11043-11062, 1994.
6. Shiah, A.; Hwang, K.S.; Wu, S.T.; and Stone, N.H.: "Three-Dimensional Simulation of Current Collection in Space," *Planet. Space Sci.*, Vol. 45, pp. 475-482, 1997.
7. Kliore, A.J.; Hinson, D.P.; Flasar, F.M.; Nagy, A.F.; and Cravens, T.E.: "The Ionosphere of Europa From Galileo Radio Occultations," *Science*, Vol. 277, pp. 355-358, 1977.
8. Spilker, T.: "Jupiter Close Polar Orbiters: Preliminary Mission Studies," Outer Planets Science Working Group Meeting Summary, September 26, 1995.

REPORT DOCUMENTATION PAGE			Form Approved OMB No. 0704-0188	
Public reporting burden for this collection of information is estimated to average 1 hour per response, including the time for reviewing instructions, searching existing data sources, gathering and maintaining the data needed, and completing and reviewing the collection of information. Send comments regarding this burden estimate or any other aspect of this collection of information, including suggestions for reducing this burden, to Washington Headquarters Services, Directorate for Information Operation and Reports, 1215 Jefferson Davis Highway, Suite 1204, Arlington, VA 22202-4302, and to the Office of Management and Budget, Paperwork Reduction Project (0704-0188), Washington, DC 20503				
1. AGENCY USE ONLY (Leave Blank)		2. REPORT DATE June 1998	3. REPORT TYPE AND DATES COVERED Technical Publication	
4. TITLE AND SUBTITLE Electrodynamic Tether Propulsion and Power Generation at Jupiter			5. FUNDING NUMBERS	
6. AUTHORS D.L. Gallagher, L. Johnson, J. Moore,* and F. Bagenal**				
7. PERFORMING ORGANIZATION NAME(S) AND ADDRESS(ES) George C. Marshall Space Flight Center Marshall Space Flight Center 35812			8. PERFORMING ORGANIZATION REPORT NUMBER M-876	
9. SPONSORING/MONITORING AGENCY NAME(S) AND ADDRESS(ES) National Aeronautics and Space Administration Washington, DC 20546-0001			10. SPONSORING/MONITORING AGENCY REPORT NUMBER NASA/TP—1998-208475	
11. SUPPLEMENTARY NOTES Prepared by Program Development Directorate *SRS Technologies, **University of Colorado				
12a. DISTRIBUTION/AVAILABILITY STATEMENT Unclassified—Unlimited Subject Category 20 Standard Distribution			12b. DISTRIBUTION CODE	
13. ABSTRACT (Maximum 200 words) The results of a study performed to evaluate the feasibility and merits of using an electrodynamic tether for propulsion and power generation for a spacecraft in the Jovian system are presented. The environment of the Jovian system has properties which are particularly favorable for utilization of an electrodynamic tether. Specifically, the planet has a strong magnetic field and the mass of the planet dictates high orbital velocities which, when combined with the planet's rapid rotation rate, can produce very large relative velocities between the magnetic field and the spacecraft. In a circular orbit close to the planet, tether propulsive forces are found to be as high as 50 N and power levels as high as 1 MW.				
14. SUBJECT TERMS tethers, electrodynamic propulsion, orbit transfer, power generation, in-space transportation			15. NUMBER OF PAGES 32	
			16. PRICE CODE A03	
17. SECURITY CLASSIFICATION OF REPORT Unclassified	18. SECURITY CLASSIFICATION OF THIS PAGE Unclassified	19. SECURITY CLASSIFICATION OF ABSTRACT Unclassified	20. LIMITATION OF ABSTRACT Unlimited	